



Simulating police containment of a protest crowd

Vector Ion Posadas and Kardi Teknomo

Abstract

This paper presents an agent-based computational model of the crowd containment tactic known as *kettling*, which involves cordons of police officers surrounding a crowd of protesters in order to restrict its movement. Our model uses steering behavior techniques to simulate a series of simple scenarios in which an unorganized group of protester agents clash with an opposing group of police agents holding position in a stationary, multiple-rank line formation. We investigate the stability and penetrability of the police formation and how they are influenced by the formation's thickness (number of layers) as well as the specific behavioral strategy employed by individual police agents—whether using global or local references, or combinations of both. Our results show that a strategy using purely global references produces optimal performance, while increasing the number of formation layers enables strategies using combined references to approach this optimum to different degrees.

Keywords

Riot control, crowd containment, *kettling*, formation control, steering behaviors

I. Introduction

Agent-based models are increasingly being used to simulate crowd behavior, ranging from the simple walking behavior of pedestrians in crowded spaces¹ to evacuation scenarios under panic conditions.² In an agent-based crowd model, each individual in the crowd is represented by an autonomous software agent that employs some method of locomotion in order to navigate its environment. A widely used approach is the rule-based technique, in which an agent applies a set of simple behavioral rules based on local information to determine its next velocity. Such rules typically include a means by which the agent moves to a desired destination and avoids collisions with obstacles or other agents. The seminal work of Reynolds³ on the flocking of “boids” showed how rule-based techniques can produce natural-looking, self-organized formation of implicit groups without a leader. He has since adapted this flocking model for generalized agents,⁴ introducing a variety of rules called *steering behaviors*, each describing a specific type of movement. Using combinations of these behaviors, agents can be made to perform a wide range of high-level tasks, depending on the needs of the model.

In this paper, we are interested in the modeling of human agents belonging to an explicit group in which the members are in a well-defined formation. Specifically, we have made use of the steering behaviors framework⁴ to

develop a simple model of the crowd containment tactic known as *kettling*, which involves cordons of police officers standing shoulder to shoulder in a tight line formation in order to block the passage of a large group of protesters (the formation used in this tactic is also analogous to the phalanx formation used in ancient warfare or to defensive lines in certain team sports, such as rugby or gridiron football). In order to simulate this coordinated formation, we introduce a new steering behavior *Formation* (a variation of the *Leader-following* behavior presented by Reynolds⁴) that steers an agent to a specified offset relative to another agent, allowing it to maintain a position directly adjacent to the reference agent. (While this paper is concerned with the simulation of a stationary line formation of agents, the utility of the *Formation* steering behavior is not limited to this application but to any group of agents maintaining a specific formation geometry, allowing for the modeling of a wide range of scenarios.) We consider different behavioral strategies to be employed by police agents in maintaining their formation—whether referencing an agent’s

Ateneo de Manila University, Quezon City, Philippines

Corresponding author:

Kardi Teknomo, Ateneo de Manila University, Loyola Heights Campus, Katipunan Avenue, Loyola Heights, Quezon City 1108, Philippines.
Email: teknomo@gmail.com

static initial position in global coordinates, or using local references to adjacent agents in conjunction with global information—and conduct simulation experiments on our model to evaluate each strategy's performance in a hypothetical scenario where the group of protesters attempts to break through and escape the kettling formation. Performance is measured using specific indices related to the formation's penetrability (based on the cumulative escapes of protester agents) and stability (based on police agents' average deviation from their ideal positions).

Our proposed model is conceptual in nature and should therefore not be judged based on the ability to make rigorous predictions regarding crowd behavior in a real-world kettling situation. Rather, its purpose is more to gain insight into the dynamics of a crowd containment scenario (e.g., determining the variables involved and the degrees to which they influence the resulting behavior), as well as to underline the potential value of using agent-based modeling in the study and development of police crowd control techniques.

The paper proceeds as follows: Section 2 gives an overview of literature regarding formation control in agent-based crowd models, followed by a summary of riot control simulators for military training applications, then by a review of the specific crowd control tactic of kettling and its use by police in the real world. Section 3 briefly describes the general architecture of our crowd model and the steering behaviors implemented. Section 4 details how the kettling scenario is defined and the design of our simulation experiments. In Section 5, we present our experiment results. In Section 6, we give a discussion of these results and conclude the paper.

2. Related work

The behavior-based approach to modeling agent formations involves the prescription of a set of elementary, locally reactive control behaviors for each agent, where each behavior has a specific low-level task such as goal-seeking, collision avoidance, or formation maintenance. These behaviors are simultaneously active and do not compete for selection—rather, a weighted combination of each behavior's desired control output determines an agent's selected action in a given moment. The flocking of “boids” in Reynolds' model³ works by combining three distinct behaviors: *Separation* for collision avoidance with neighboring agents; *Cohesion* to move toward the average position of neighboring agents; and *Alignment* to steer toward the average heading of neighboring agents. The combination of these behaviors using strictly local information results in a moving, albeit unstructured, formation of agents while avoiding collisions. Tanner et al.⁵ proposed a variant flocking model in which agents have a determinate place within the group formation based on a

connected graph that defines an explicit set of “preferred” neighbors for each agent.

The control of mobile robots in well-defined formation geometries has also been dealt with using the behavior-based approach. A study by Monteiro and Bicho⁶ proposed using nonlinear attractor dynamics to model the control architecture that enables a group of three robots to move in triangular formation while avoiding obstacles. Yun et al.⁷ presented a number of behavior-based algorithms that enables a group of physical, non-holonomically constrained mobile robots to arrange themselves in a line or circle formation. Balch and Arkin⁸ presented a behavior-based mechanism controlling a small group of robots to navigate an obstacle-laden environment while maintaining one of four possible formations: line, column, diamond, and wedge. Different techniques for formation referencing are also considered: *leader-reference*, *unit-center reference*, and *neighbor-reference*. They demonstrated the performance of their mechanism using mobile robots in the laboratory as well as unmanned ground vehicles (UGVs) in the field.

While these studies among numerous others propose solutions for formation control in a small group of mobile robots, the problem of formation control in large groups of human-like agents is less explored. Takahashi et al.⁹ proposed a method of formation control using spectral graph theory. They demonstrated how their method can be used to animate a marching band in transitioning formations, tactical formations in a soccer game, and as artistic formations of a large crowd of individuals.

The use of agent-based models to simulate scenarios related to riot control has been explored in a number of studies, most notably in the context of non-combat military operations. Varner et al.¹⁰ have developed a training simulator for use by the United States Marine Corps to train squad leaders for non-combat peacekeeping missions. The simulator provides the trainee with a simulated urban environment wherein they must interact in real-time with a crowd of locals that respond to the trainee's actions. Given a specific situation background and rules of engagement for the training exercise, the trainee is tasked with pacifying the crowd by inputting actions such as issuing verbal instructions to the crowd or employing lethal or non-lethal munitions. Upon resolution of the situation, the trainee's actions are reviewed by an instructor. More recently, McKenzie et al.¹¹ are in the process of developing an interactive crowd simulation for real-time tactical training in a variety of military mission scenarios involving crowds of non-combatants. Their simulation is designed to be interoperable with existing military simulations and makes use of commercial gaming technology to render the urban terrain and the physical behaviors of the crowd. They also intend to draw on various psychological studies as the basis for the cognitive model of the crowd's behavior.

With regard to the specific crowd control tactic of kettleing used by law enforcement, to our knowledge, there are no existing studies that deal with its modeling through computer simulation. In this regard, this paper presents a novel area of research. Kettling is defined as “a police method for management of large demonstrations,” in which “cordons of police contain a crowd within a limited area.”¹² Use of the tactic has seen a rise in recent years despite much controversy surrounding its legality and indiscriminate use by police.¹³ The earliest documented use of the tactic occurred in 1986 when police in Hamburg, Germany, cordoned and detained more than 800 protesters for up to 13 hours.¹⁴ In this instance, the kettle formation was stationary. However, kettleing can take on a mobile form where police position themselves to surround an entire group of protesters as it marches, controlling its route and starting and stopping at will. This type of kettle, known in Germany as *wanderkessel* (“wander kettle”), saw use again by Hamburg police in 2007.¹⁵ In order to maintain such a dynamic form of control, large numbers of police are necessary—possibly outnumbering the protesters. A more recent variation of kettleing called “bridge kettle” involves police using the mobile kettle to force the march of a group of protesters toward a large bridge on top of an urban river, where the kettle formation stops and the protesters are detained. In this case, the surrounding water serves as a barrier to individuals attempting to escape. This type of kettle was seen on the Guillotière bridge in Lyons, France, and on Westminster Bridge in London, UK, both in 2010.¹⁵ Yet another type of kettle known as “hyper kettle” involves the surrounding police cordons progressively reducing the confinement area to a smaller space, compressing the protesters against each other and any available structures. This type of kettle was used by British police on protesters in Bolton, UK, in 2010.¹⁵

3. Framework

Our model operates under the aforementioned steering behaviors framework of Reynolds⁴ and extends the work of Schnellhammer and Feilkas,¹⁶ who have authored a Java build of the basic agent model in Reynolds’ framework. In this framework, the behavior of an agent is composed of three layers: *action-selection*, *steering*, and *locomotion*. The first layer determines what steering behaviors are employed by the agent based on its top-level scenario-specific goals; the second layer determines the agent’s velocity at a given timestep, computing the overall force vector from the individual steering forces produced by the agent’s active steering behaviors; the third layer updates the agent’s position in the simulation environment based on its computed velocity. Each steering behavior is

qualified to a certain type of force \mathbf{f}_j with weight w_j to produce the resultant force \mathbf{f}_i of each agent i :

$$\mathbf{f}^i = \sum_j w_j^i \mathbf{f}_j^i \quad (1)$$

Behaviors that take the presence of nearby agents into account have a *radius* attribute, which determines the size of the local neighborhood from which to search for relevant agents. This radius roughly translates to the real-world idea of a “personal bubble” extending from an individual, within which intrusions by other persons provoke a reaction in the individual¹⁷—for example, by altering its walking trajectory to avoid a collision.

The simulation environment is an empty two-dimensional space that is closed on all sides; hence, the edges represent impassable walls. Each agent in our model is represented by a filled circle whose diameter represents the shoulder breadth of an adult human, which we have taken to be 0.5 m and is homogeneous for all agents. The fill color of the circle represents the agent’s group membership. A small black triangle at the edge of the circle points to the direction of the agent’s steering force in a given timestep. Each agent has the attributes V_{\max} for its maximum velocity, F_{\max} for its maximum acceleration, and m for its mass. We have fixed V_{\max} to a unit vector and F_{\max} to a magnitude of 0.2 for all agents, while m is normalized to be fixed to one unit. Based on our assumed value of 0.5 m for the agent diameter and a typical value for human walking speed of 1.3 m/s,¹⁸ we have calibrated our agent model such that one simulation second represents the time interval in which a lone, unhindered agent can move a distance of 1.3 m in the simulation space.

Each agent holds a static list of steering behaviors that it employs. At every simulation timestep, each active steering behavior in the list produces a steering force vector scaled by the respective behavior’s weight before they are summed to obtain the total steering force, whose length is then truncated to the agent’s maximum force F_{\max} and divided by the agent’s mass m to get the agent’s acceleration. This acceleration is added to the agent’s current velocity, truncated by the agent’s maximum velocity V_{\max} to get its new velocity, which is then used to update its position in the simulation space.

Steering behaviors used in our model are *Seek*, *Separation*, and *Formation*. The first two are implemented as defined by Reynolds.⁴ The following is a brief description of each of these behaviors as well as variations used in our model.

1. *Seek*: this behavior allows steering to a specified static target position in global space. The steering force is based on the current velocity of the agent and the position of its target. The desired velocity

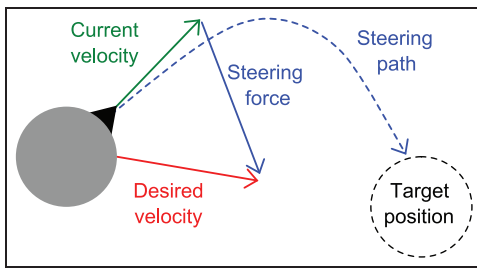


Figure 1. The steering force produced by the *Seek* behavior is the vector difference between the agent's desired velocity (the vector pointing from the agent to the target position) and its current velocity, as given by Helbing et al.²

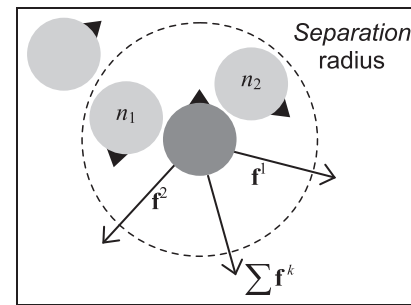


Figure 2. The steering force produced by the *Separation* behavior is the vector sum of the repulsive forces generated from each neighboring agent within the behavior's radius.

of an agent is expressed as a vector pointing from the agent to the target, scaled to the agent's maximum velocity. The current velocity of the agent is then subtracted from the desired velocity to get the resulting steering force. If $\mathbf{p}^i(t)$ and $\mathbf{v}^i(t)$ are the current position and current velocity of agent i , and $\mathbf{e}(t)$ is the target position, then the *Seek* steering force (as illustrated in Figure 1) is given by

$$\mathbf{f}_{\text{Seek}}^i(t) = V_{\max}^i \frac{\mathbf{e}(t) - \mathbf{p}^i(t)}{\|\mathbf{e}(t) - \mathbf{p}^i(t)\|} - \mathbf{v}^i(t) \quad (2)$$

Our model also makes use of a modified *Seek* behavior *EdgeSeek*, which produces a steering force in the direction perpendicular to a specific edge of the environment from the given agent, that is, an agent i at position $\mathbf{p}^i(t)$ with coordinates (x^i, y^i) at time t using *EdgeSeek* will have a target position $\mathbf{e}(t)$ with coordinates (x_{\min}, y^i) if seeking the left edge, (x_{\max}, y^i) if seeking the right edge, (x^i, y_{\min}) if seeking the top edge, or (x^i, y_{\max}) if seeking the bottom edge, toward which the agent is steered using (2).

2. *Separation*: this behavior enables an agent to maintain a certain distance from other agents by means of a repulsive force from the direction of each nearby agent within the behavior's radius. The repulsive force vector is obtained by subtracting the position of the nearby agent from the computing agent. Multiple repulsive forces from several nearby agents are combined to produce the overall steering force (Figure 2). In our model, this behavior is used to produce the pushing effect generated by collisions between agents rather than for collision avoidance. This is implemented by setting the behavior's radius to twice the agent radius (i.e., the computing agent will only react via *Separation* to a neighboring agent if the distance between their circumferences is zero). If superscript k represents nearby agents, then the

Separation steering force is given by

$$\mathbf{f}_{\text{Separation}}^i(t) = V_{\max}^i \sum_k \left(\frac{2r}{\|\mathbf{p}^i(t) - \mathbf{p}^k(t)\|} - 1 \right) \left(\frac{\mathbf{p}^i(t) - \mathbf{p}^k(t)}{\|\mathbf{p}^i(t) - \mathbf{p}^k(t)\|} \right) \quad (3)$$

Our model also has distinct variants of *Separation* for in-group agents and out-group agents—the former only considers neighboring agents belonging to the same group, while the latter only considers neighboring agents not from the same group. The two variants can be active concurrently and can have differing weights and radii. Finally, our model makes use of a *Separation* behavior with respect to a closed edge of the environment, producing an inward repulsive force perpendicular to the length of the edge.

3. *Formation*: this behavior is implemented as an offset *Seek* to a reference agent. The offset is a vector in local coordinates, defined by the initial displacement between the actor agent and the reference agent in the kettling formation. The steering force produced by the *Formation* behavior is a *Seek* force directed toward the offset point relative to the current position of the reference agent (Figure 3). Hence, if $\mathbf{p}^i(t)$ and $\mathbf{p}^r(t)$ are the positions of the actor agent i and the reference agent r at time t , then the target position $\mathbf{e}(t)$ for the *Seek* force as defined in Equation (2) is given by

$$\mathbf{e}(t) = \mathbf{p}^r(t) + (\mathbf{p}^r(0) - \mathbf{p}^i(0)) \quad (4)$$

Multiple *Formation* behaviors referencing different target agents can be concurrently active for a single agent. This usage of the *Formation* behavior allows us to develop different strategies for groups of agents to maintain their specific formation geometry. These formation strategies are described in detail in the next section.

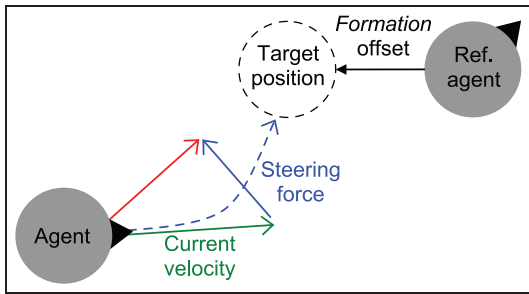


Figure 3. The steering force produced by the *Formation* behavior is a Seek steering force directed toward the position of a specific reference agent with an added offset.

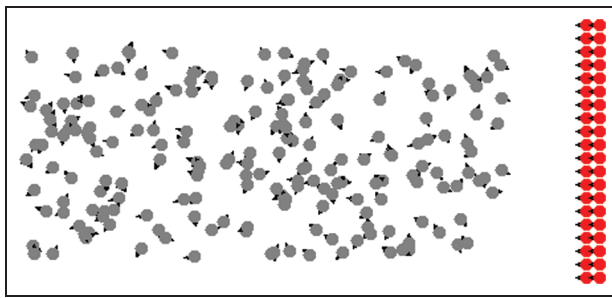


Figure 4. Initial state of the kettle scenario, showing a crowd of 200 protester agents on the left and a two-rank formation of police agents on the right, with 20 agents in each rank.

4. Scenario and experiment design

The kettle scenario takes place in a closed-border rectangular area 25 m long and 10 m wide, and involves two types of agents: *police* and *protester*. Police agents are red in color and stand side by side (with no spaces in between) in a stationary, multiple-rank line formation on the right-hand side of the environment. Their top-level goal is to stay in place within their formation in accordance with the designated formation strategy (to be detailed later in this section). Protester agents are gray in color and have randomly determined initial positions on the left-hand side of the environment, at least 3 m away from the front-most rank of the police formation. They act individually (i.e., they have no regard for other protester agents other than reacting to collisions with them), but have a common top-level goal of moving toward any point on the right-hand edge of the environment, upon reaching which they are removed from the simulation. The initial state of the kettle scenario is shown in Figure 4.

Protester agents use the *Separation* and *EdgeSeek* behaviors with arbitrarily chosen weights of 95 and 5, respectively. The separation radius is set to twice the agent radius. Police agents, on the other hand, have distinct

Separation behaviors for the in-group and out-group, each having a weight of 40 but the former having a minuscule negative radius such that separation between police agents only occurs when there is at least a one-pixel overlap between them. This is to allow police agents to stand directly adjacent to each other without provoking a collision reaction. We have set the behavior weights thusly based on preliminary experiments on the model, finding suitable values that visually minimize overlapping between agents (occurring when *Separation* weights are too weak) and such that protester agents are generally overpowered by police agents but still exhibit an impulse to move to the goal edge.

The steering behaviors to be used by police agents for formation control are determined by the formation strategy being employed by the group. A formation strategy consists of one or more components among **SP** (static position reference), **FF** (frontal formation reference), and **LF** (lateral formation reference). Each component is simply a stipulation of a natural reference point by an individual police agent for maintaining proximity and alignment with other police agents in a multilayer cordon: the **SP** component stipulates a *Seek* behavior targeting the agent's initial position in global space; hence, the formation is maintained by way of police agents attempting to stay in their designated positions within the kettle formation. The **FF** component stipulates a *Formation* behavior referencing the adjacent agent to its front; that is, police agents attempt to maintain positional alignment with agents directly in front of them. This component acts like a glue connecting multiple ranks within the formation. The **LF** component stipulates two *Formation* behaviors referencing lateral adjacent agents; that is, police agents will attempt to maintain positional alignment with the agents directly to their left and right. This component acts like a glue between police agents in the same rank. The steering forces and corresponding targets associated with each component are illustrated in Figure 5.

Deriving from these three components, we have defined six formation strategies: **SP**, **FF**, **FF + SP**, **LF + SP**, **FF + LF**, and **FF + LF + SP**. These six strategies comprise an exhaustive set of possible combinations of the three components (excluding the strategy consisting of the **LF** component by itself, which is not viable for the purposes of this paper as it lacks the means for the police agents to maintain the inter-rank structural integrity of the kettle formation). The formation control behaviors prescribed by each strategy are described in Table 1. In all strategies, police agents on the front-most rank always use the *Seek* behavior targeting their initial positions in order for the entire group to remember its ideal position in the simulation space. Thus, police agents on the front-most rank can be considered as leaders for the purpose of the group's formation control. Police agents on succeeding ranks can either reference adjacent police agents in front

Table I. The six strategies to be employed by police agents for maintaining the structure of the kettle formation, with the corresponding formation control behaviors described.

Formation strategy	Description of formation control behaviors
Static position reference (SP)	All agents use <i>Seek</i> targeting their designated initial positions within the kettle formation.
Frontal formation reference (FF)	Agents in the front-most rank use <i>Seek</i> targeting their initial positions. Agents in succeeding ranks use <i>Formation</i> referencing the adjacent agents to their front (in the previous rank).
Frontal formation + static position reference (FF + SP)	All agents use <i>Seek</i> targeting their initial positions. Agents in succeeding ranks use <i>Formation</i> referencing the adjacent agents to their front.
Lateral formation + static position reference (LF + SP)	All agents use <i>Seek</i> targeting their initial positions and <i>Formation</i> referencing the adjacent agents to their left and right.
Combined formation reference (FF + LF)	Agents in the front-most rank use <i>Seek</i> targeting their initial positions and <i>Formation</i> referencing adjacent agents to their left and right. Agents in succeeding ranks use <i>Formation</i> referencing the adjacent agents to their front, left, and right.
Combined formation + static position reference (FF + LF + SP)	Agents in the front-most rank use <i>Seek</i> targeting their initial positions. Agents in succeeding ranks use <i>Formation</i> referencing adjacent agents to their front. All agents use <i>Formation</i> referencing adjacent agents to their left and right.

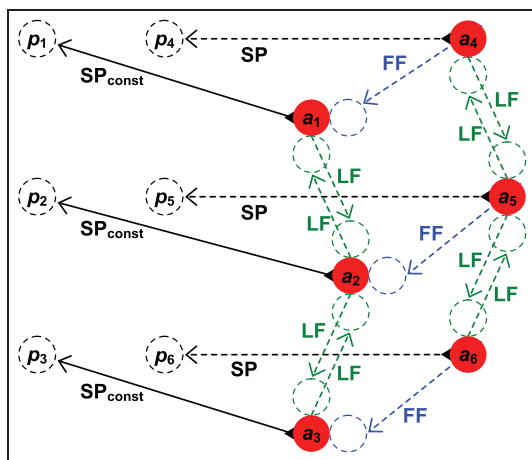


Figure 5. A 2-rank formation with three police agents (filled circles) in each rank, showing the steering forces involved in each formation strategy component. Agents a_1 to a_3 are on the front-most rank while agents a_4 to a_6 are on the subsequent rank. Each arrow labeled **SP**, **FF**, or **LF** shows the direction of a steering force that is active when the formation strategy being employed has the respective component label in its name. **SP** forces steer toward agents' initial positions while **FF** and **LF** forces have targets that move with their reference agents. The **SP_{const}** forces of agents on the front-most rank (solid arrows) are always active in all strategies

of them or laterally using *Formation* and/or also use *Seek* to their initial positions.

The specific combination of formation control behaviors used by a police agent depends on the formation

strategy being employed as well as the agent's position within the kettle formation—whether it is in the front-most rank or succeeding ranks, and whether it is positioned at the middle or the end of the rank. In any particular case, a total weight of 20 is divided equally among the set of behaviors prescribed (see Figure 6).

We conducted simulation experiments on our model using these six formation strategies for the police agents as well as varying the number of ranks in the formation from two to five. A single experiment run terminates after 600 s in simulation time or when all protester agents have escaped the environment. At each simulation timestep, the following performance indices are recorded.

1. The protester crowd remainder R_t is defined by the equation

$$R_t = R_0 - E_t \quad (5)$$

where R_0 is the initial number of protester agents and E_t is the cumulative number of protester agents that have escaped (i.e., reached the right-hand edge of the environment) at time t . This index provides a measure of the kettle formation's penetrability based on its rate of decrease and its value when the index is in equilibrium over t ; the latter providing an approximation of the maximum protester crowd size that the particular kettle formation can contain indefinitely. A lower rate of decrease and higher equilibrium value in this index indicates better performance (less penetrability).

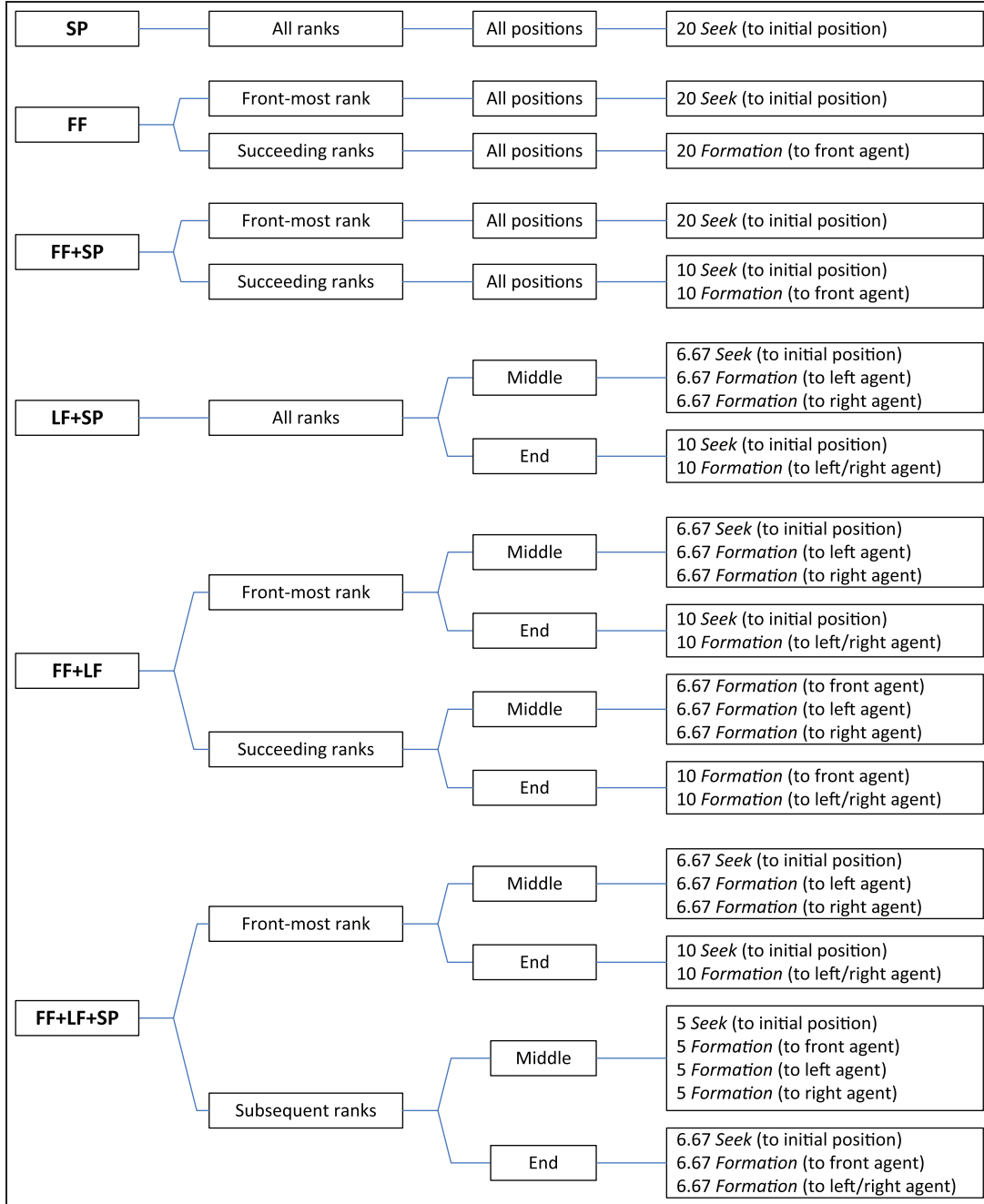


Figure 6. The set of steering behaviors used by a given police agent for formation control is determined by the formation strategy being employed and the position of the agent within the formation, with a total weight of 20 distributed equally among the different behaviors.

2. The mean formation deviation D_t of police agents is defined by the equation

$$D_t = \frac{\sum_{i=1}^n \sqrt{(x_{i0} - x_{it})^2 + (y_{i0} - y_{it})^2}}{n} \quad (6)$$

which is the average of the distance (in meters) of each police agent i from its initial position (x_{i0}, y_{i0}) at time t over all n police agents. This index provides a measure of the stability of the kettle formation based on how far police agents are displaced from their initial positions on average, with lower values indicating better performance.

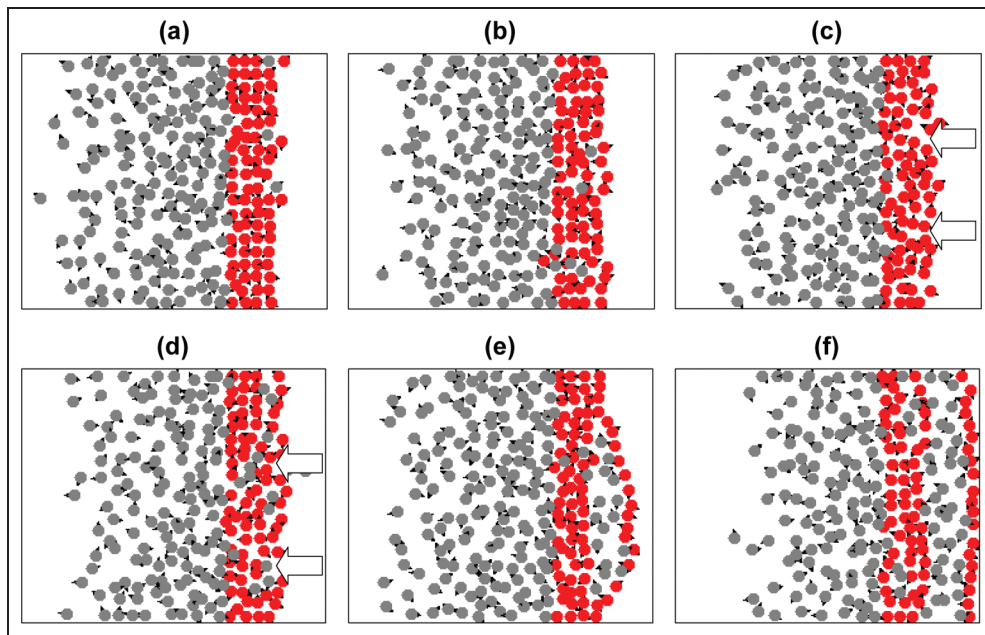


Figure 7. Snapshots of the simulation at 120 s using different formation strategies, showing penetration of the police kettling formation by the protester crowd. (a) The **SP** strategy shows highly stable formation ranks with very low penetrability. (b) The **FF + SP** strategy shows slightly uneven ranks but a similar degree of impenetrability. (c) The **FF** strategy shows broken ranks of agents as well as the appearance of fissures along the depth of the formation (indicated by arrows). (d) The **FF + LF + SP** strategy shows uneven but still discernible ranks of agents and the appearance of fissures along the length of the formation (indicated by arrows). (e) The **LF + SP** strategy shows significant deformation in the formation ranks, particularly in the rearmost rank, which often manifests a bulge within in which several protester agents are trapped. (f) The **FF + LF** strategy shows extreme deformation and positional displacement in the formation ranks, with the rearmost rank often getting separated from the front ranks by a large group of protester agents that extends the entire length of the formation.

A sustained value close to 0 m in this index indicates a highly stable formation, since a value of 0 m implies all police agents are exactly in their initial positions. In plotting this index, we take its time average for smoothing purposes.

5. Results

Setting the number of formation ranks to four and the initial size of the protester crowd to 200, we have tested our model using the six different formation strategies described in Section 4. Firstly, we will discuss our observations regarding the behavior of the kettling formation in each strategy, followed by an analysis of their quantifiable performance with respect to the measures stated previously in Section 4.

Visually, the **SP** strategy produces the most stable formation, followed closely by **FF + SP** then by **FF**. In these three strategies, the entirety of the kettling formation is generally able to hold its initial position in the simulation space. In the **SP** strategy, the ranks of the formation are clearly visible at any given time, remaining mostly straight and unbroken (Figure 7(a)). The **FF + SP** strategy shows slight deformations in the ranks, particularly in the initial

stages when the protester crowd is at its maximum, but eventually exhibits similar behavior to **SP** as the protester crowd decreases in size (Figure 7(b)). On the other hand, the ranks of the formation produced by the **FF** strategy are mostly crooked even in the latter stages. Narrow fissures along the depth (longitudinal dimension) of the formation can also be seen (Figure 7(c)).

The remaining three formation strategies, namely **LF + SP**, **FF + LF**, and **FF + LF + SP**, share the common characteristic of having a lateral formation reference component. Visually, **FF + LF + SP** appears to be the most stable of the three, followed by **LF + SP**, then by **FF + LF**. In **FF + LF + SP**, the ranks of the formation can get very crooked, especially the rearmost rank. Also, the emergence of fissures along the length of the formation (between two ranks) can sometimes be seen, trapping protester agents in small pockets within the formation (Figure 7(d)). In **LF + SP**, these pockets of trapped protester agents can become much larger, often evolving to a single large pocket that deforms the rearmost rank of the formation into a bulge (Figure 7(e)). Finally, the **FF + LF** strategy visibly produces the least stable formation among all strategies. Upon initial contact with the escaping protester crowd, the entire formation of police agents is

Table 2. Containable protester crowd size after 600 s using different formation strategies and increasing number of ranks. Each value is taken from the arithmetic mean of five experiment runs, with standard deviation in parentheses. Shaded cells show values that meet the threshold of 100 protester agents contained.

Formation strategy	Protester crowd remainder after 600 s (initial value of 200)			
	2 ranks	3 ranks	4 ranks	5 ranks
SP	99.6 (1.67)	110.2 (3.35)	120.4 (2.79)	124.0 (3.32)
FF + SP	99.8 (4.97)	105.6 (2.97)	109.4 (3.91)	111.4 (2.97)
FF	93.2 (1.92)	95.8 (3.83)	98.8 (3.56)	97.4 (6.11)
LF + SP	67.6 (5.03)	87.6 (2.30)	102.2 (1.92)	108.8 (3.56)
FF + LF + SP	72.4 (1.52)	86.6 (4.98)	91.8 (2.59)	104.4 (3.65)
FF + LF	66.2 (1.79)	79.0 (4.69)	77.8 (4.32)	83.4 (3.36)

pushed to the edge of the simulation space, whereupon the front ranks start to recover to their ideal positions. The rearmost rank, however, is usually unable to do the same and remains trapped near the edge, creating a layer of protester agents that extends the entire length of the formation, sandwiched between the rearmost rank and the front ranks (Figure 7(f)). This pattern persists until the number of protester agents in this layer decreases, at which point the rearmost rank begins to reclaim its position behind the front ranks. This emergent property of the **FF + LF** strategy in which the rearmost rank gets separated from the front ranks can be observed using any number of ranks from two to five.

5.1. Crowd remainder

As noted previously, the protester crowd remainder R_t is the initial number of protester agents R_0 minus the cumulative number of protester agents that have escaped at time t . The rate of decrease as well as the final value of this index for a given formation strategy provide an indication of the degree of penetrability of the formation produced by the strategy in comparison with others. In 2-rank formations with an initial protester crowd size R_0 of 200 (Figure 8), we can see that the **SP** and **FF + SP** strategies are the two best performers and actually have similar performance. They are followed by the **FF** strategy, which performs slightly worse; then there is a large gap in performance to the remaining three strategies, **FF + LF + SP**, **LF + SP**, and **FF + LF** (in order of decreasing performance), showing that strategies with the lateral formation reference component are more easily penetrated by the protester agents.

When the number of ranks is increased to five while keeping the initial protester crowd size to 200, all strategies show improved performance; however, some strategies show better improvement than others. The **SP** strategy now outperforms the **FF + SP** strategy by a large margin, and the **FF** strategy is now outperformed by the **LF + SP** and **FF + LF + SP** strategies, leaving the **FF + LF** strategy as still the worst performer. Comparing the crowd

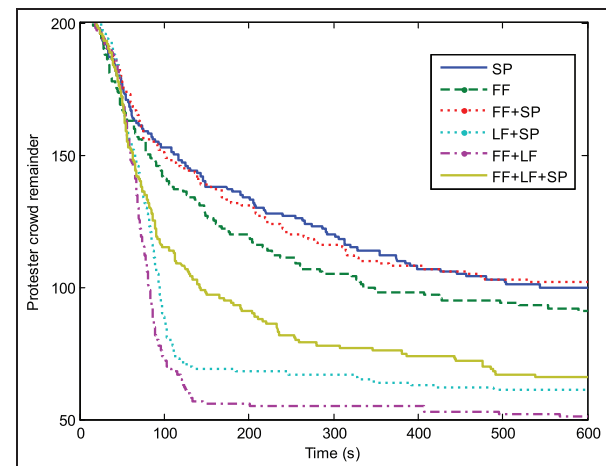


Figure 8. Crowd remainder index in 2-rank formations using different strategies, showing a large disparity in performance between strategies with the lateral formation reference (**LF**) component and those without.

remainder index in increasing ranks of the different formation strategies (Figure 9), we see very little change in the performance of the **FF** and **FF + SP** strategies, while there is a particularly large improvement in the performance of the **LF + SP**, **FF + LF**, and **FF + LF + SP** strategies with an increase from two to three ranks. In other words, an increase in the number of ranks has smaller effect on strategies with the frontal formation reference (**FF**) component but a larger effect on strategies with the lateral formation reference (**LF**) component. In all strategies, however, an increase from four to five ranks shows minimal improvement, suggesting that increasing the number of ranks beyond four grants diminishing returns on performance gain in this index.

Table 2 shows the maximum protester crowd size that the kettle formation can contain over a period of 600 s using different formation strategies and increasing number of ranks. In order to contain a protester crowd size of 100, the number of formation ranks necessary using the **SP** or

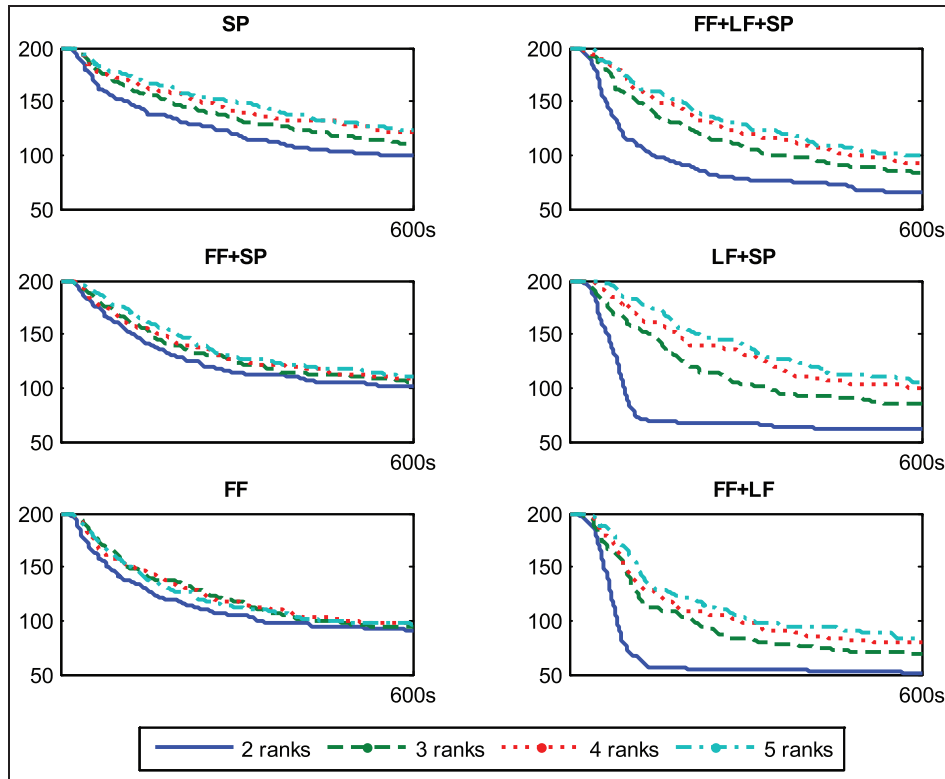


Figure 9. Each sub-chart shows the crowd remainder performance index over time for the respective formation strategy in two to five ranks. **FF + SP** and **FF** show very little performance gain with an increase in ranks, while strategies with the **LF** component (**FF + LF + SP**, **LF + SP**, and **FF + LF**) show larger performance gains, particularly with an increase from two to three ranks. In all strategies, increasing the number of ranks beyond four shows minimal performance gain.

FF + SP strategies is three; four ranks are required if using the **LF + SP** strategy, and five ranks are required if using the **FF + LF + SP** strategy. Five formation ranks using either the **FF** or **FF + LF** strategies are not enough to contain a crowd size of 100.

5.2. Mean formation deviation

The mean formation deviation D of police agents provides an indication of the stability of the kettle formation over time t . In 2-rank formations (Figure 10), the **SP**, **FF + SP**, and **FF** strategies show very minimal deviation (in that order of decreasing performance) compared to the **FF + LF + SP**, **LF + SP**, and **FF + LF** strategies (in that order of decreasing performance), each of which show a peak in deviation in the initial stages followed by a gradual decline as the protester crowd size decreases. This result is consistent with the observed stability of formations produced by the former three strategies and quantifiably demonstrates the extreme instability of the latter three strategies, all of which have the lateral formation reference (**LF**) component.

As the number of formation ranks is increased, the performance of the **LF + SP** and **FF + LF + SP** strategies

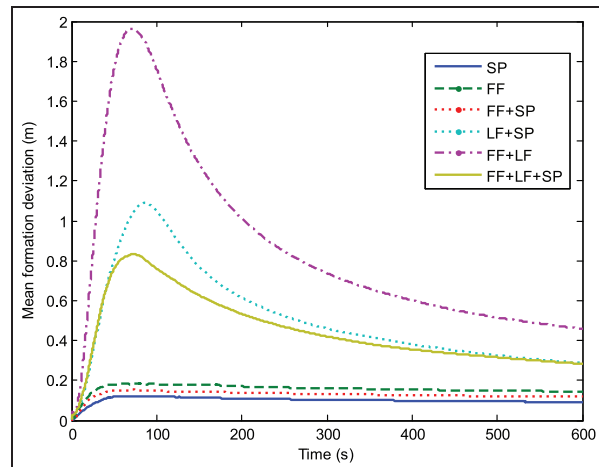


Figure 10. Mean formation deviation of police agents in 2-rank formations using different formation strategies, showing the variation of performances. Strategies that have the lateral formation reference (**LF**) component exhibit extreme instability compared to those that do not.

improve dramatically, and in fact when the number of formation ranks is increased to five, they show similar performance to the **FF** strategy. However, the **SP** and **FF + SP**

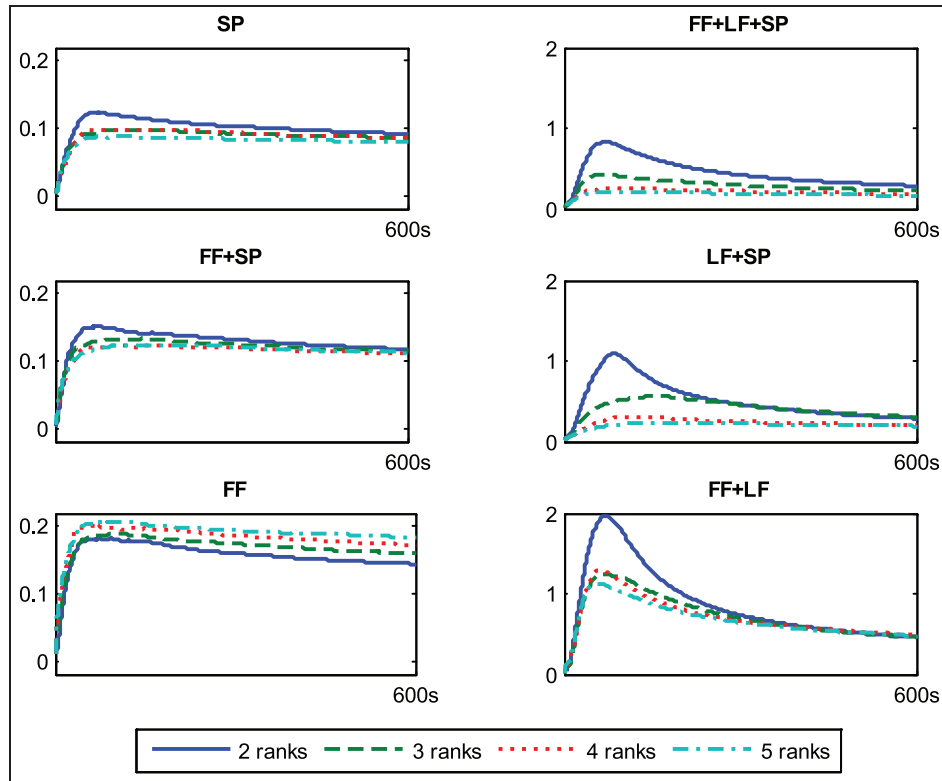


Figure 11. Each sub-chart shows the mean formation deviation performance index (in meters) over time for the respective formation strategy in two to five ranks (note the larger scale of the y-axes on the right-hand column). **SP** and **FF + SP** are very stable and show little improvement in performance from three ranks onward. **FF**, while also very stable, shows worsening performance with an increase in ranks. Strategies with the **LF** component show extreme instability in 2-rank formations, but at 4 ranks, **FF + LF + SP** and **LF + SP** show similar performances to the strategies in the left-hand column. **FF + LF** also shows improving performance with an increase in ranks, but not to the same degree as the previous two strategies.

strategies still perform the best while the **FF + LF** strategy still performs the worst. Looking at the mean formation deviation index in increasing ranks of the different formation strategies (Figure 11), we can see that after a peak in the initial stages (the size of which varies with ranks), the deviation gradually evens out to roughly the same value regardless of ranks. This behavior is exhibited by all strategies except the **FF** strategy, which oddly shows slightly worsening performance with each rank increase. Strategies with the lateral formation reference (**LF**) component show extreme instability at two ranks, but the aforementioned dramatic improvement of **LF + SP** and **FF + LF + SP** can be seen even at four ranks, at which point they show deviation indices an order of magnitude smaller. These results indicate that while having the **LF** component makes a formation strategy unstable, having the **SP** component as well allows it to become very stable with an increase in ranks. A strategy with the **FF** component by itself actually shows slightly deteriorating stability with an increase in ranks, but combination with other components overrides this peculiar behavior.

Table 3 shows the mean deviation of police agents from their ideal positions in the kettle formation after 600 s, using different formation strategies and an increasing number of ranks. Based on the differences in values, we can categorize the strategies into three brackets of stability performance. The **SP** strategy is alone in the most stable bracket, while the **FF**, **FF + SP**, **LF + SP**, and **FF + LF + SP** strategies fall in the middle bracket, showing comparable performances in any number of ranks. Lastly, the **FF + LF** strategy is alone in the least stable bracket.

6. Conclusion

In this paper, we have presented a behavior-based agent model of the crowd containment tactic known as kettle, in which a multiple-rank line formation of police officers blocks the passage of a group of aggressive protesters. We examined the performance of the kettle formation (in terms of formation stability and penetrability by protester agents) using different strategies for the formation

Table 3. Mean formation deviation of police agents after 600 s using different formation strategies and increasing number of ranks. Each value is taken from the arithmetic mean of five experiment runs, with standard deviation in parentheses. Each different shade background shows a potential grouping of formation strategies based on similarity of performance in terms of formation stability.

Formation strategy	Mean formation deviation of police agents after 600 s (in cm)			
	2 ranks	3 ranks	4 ranks	5 ranks
SP	7.4 (0.3)	8.2 (0.5)	7.3 (1.2)	6.3 (0.8)
FF + SP	9.0 (1.5)	9.7 (1.2)	10.3 (0.9)	10.1 (0.4)
FF	13.8 (3.0)	13.2 (3.0)	16.6 (2.9)	16.6 (1.2)
FF + LF + SP	10.6 (3.1)	12.4 (2.5)	13.3 (3.0)	13.8 (0.8)
LF + SP	13.5 (2.4)	13.2 (1.9)	12.6 (1.6)	13.4 (1.3)
FF + LF	22.6 (6.2)	26.4 (4.8)	22.3 (3.7)	29.6 (5.9)

maintenance behaviors of police agents. Our results show that a formation strategy where police agents each reference a designated static position within the formation irrespective of other police agents (**SP**) produces optimum performance in both measures (i.e., high stability and low penetrability). A strategy that combines static position referencing and forward alignment maintenance behaviors (**FF + SP**) performs comparably to the purely static position-based strategy, whereas a strategy using forward referencing exclusively (**FF**) does not perform as well and shows very little improvement in performance even when the number of formation layers is increased. On the other hand, a strategy that combines static position referencing with lateral alignment maintenance behaviors (**LF + SP**) shows even worse performance in thin formations, but this performance shows considerable improvement with an increase in formation layers, approaching similar performance to the purely static position-based strategy in thick formations. A full combination strategy using static position referencing as well as both forward and lateral referencing (**FF + LF + SP**) follows a very similar pattern, showing just slightly better performance than the former in thin formations. Lastly, a strategy consisting of both forward and lateral alignment maintenance behaviors but without static-position referencing (**FF + LF**) shows the worst performance among all the strategies. Moreover, while increasing formation thickness results in lower penetrability for this strategy, it creates very little improvement in terms of stability, with entire ranks of the formation invariably becoming completely displaced by the protester crowd even in thicker formations.

Future directions for this research will consist of the exhaustive exploration and sensitivity analysis of formation control behavior weightings in order to fully evaluate the disparities in performance produced by different types of formation referencing. More significantly, our results require validation—possibly by way of real-world experiments involving human subjects instructed to form a cordon and to maintain its integrity by attempting to remain

in physical contact with adjacent individuals in the cordon, as specified in the different formation strategies used in our model. Such experiments will serve to refine the behavior of our model to more closely reflect the empirical data. Additional refinements to the model will include more complex agent behaviors and scenario definitions that will allow the simulation of variant kettle types. Pursuing these steps will be crucial in order to realize the model's long-term potential for development into a computational tool that can aid in the training of various police forces in more effective crowd containment techniques.

Funding

This work was supported by the Philippine Council for Industry, Energy, and Emerging Technology Research and Development Department of Science and Technology (PCIEERD-DOST) and the Philippine Higher Education Research Network (PHERNET).

References

- Helbing D, Farkas IJ, Molnár P and Vicsek T. Simulation of pedestrian crowds in normal and evacuation situations. *Pedestrian Evacuation Dyn* 2002; 21: 21–58.
- Helbing D, Farkas I and Vicsek T. Simulating dynamical features of escape panic. *Nature* 2000; 407: 487–490.
- Reynolds C. Flocks, herds and schools: a distributed behavioral model. *Comput Graph* 1987; 21: 25–34.
- Reynolds C. Steering behaviors for autonomous characters. In: *Proceedings of the game developers conference*, San Jose, CA, US, 1999, pp.763–782.
- Tanner HG, Jadbabaie A and Pappas GJ. Stable flocking of mobile agents part I: fixed topology. In: *Proceedings of the 42nd IEEE conference on decision and control*, Maui, HI, US, 2003, pp.2010–2015.
- Monteiro S and Bicho E. A dynamical systems approach to behavior-based formation control. In: *Proceedings of the IEEE international conference on robotics and automation*, Washington, DC, US, 2002, pp.2606–2611.
- Yun X, Alptekin G and Albayrak O. Line and circle formation of distributed physical mobile robots. *J Robot Syst* 1997; 14: 63–76.

8. Balch T and Arkin RC. Behavior-based formation control for multi-robot teams. *IEEE Trans Robot Autom* 1998; 14: 926–939.
9. Takahashi S, Yoshida K, Kwon Y, et al. Spectral-based group formation control. *Comput Graph Forum* 2009; 28: 639–648.
10. Varner D, Royse SD, Micheletti J, et al. USMC small unit leader non-lethals trainer (SULNT). In: *Proceedings of the international training equipment conference*, 1998.
11. McKenzie FD, Petty MD, Kruszewski PA, et al. Integrating crowd-behavior modeling into military simulation using game technology. *Simulat Gaming* 2008; 39: 10–38.
12. Scorer R. Kettling matters. *New Law J* 2011; 161, <http://www.newlawjournal.co.uk/nlj/content/kettling-matters>.
13. Joyce P and Wain N. *Palgrave dictionary of public order policing, protest and political violence*. New York: Palgrave Macmillan, 2014.
14. Hudig K. The growing use of “preventative” arrests. *Statewatch J* 2010; 20: 4–6.
15. Sørli S. The political aesthetics of police kettling. *Tripwire A J Poetics* 2014; 8: 139–150.
16. Schnellhammer C and Feilkas T. The SteeringBehaviors Webpage, <http://www.steeringbehaviors.de> (accessed 6 December 2015).
17. Hall ET. *The hidden dimension*. New York: Anchor Books, 1990.
18. Knoblauch RL, Pietrucha MT and Nitzburg M. Field studies of pedestrian walking speed and start-up time. *Transp Res Rec J Transp Res Board* 1996; 1538: 27–38.

Author biographies

Vector Ion Posadas has a master's degree in computer science from the Ateneo de Manila University, Philippines. He is currently working at the same university as a research assistant for the Pedestrian and Traffic Computing Laboratory of the Department of Information Systems and Computer Science. His research interests include crowd simulation and machine learning.

Kardi Teknomo is an associate professor and head of the Pedestrian and Traffic Computing Laboratory in the Department of Information Systems and Computer Science, Ateneo de Manila University, Philippines. His personal website is <http://people.revoledu.com/kardi/>.